Journal Pre-proofs

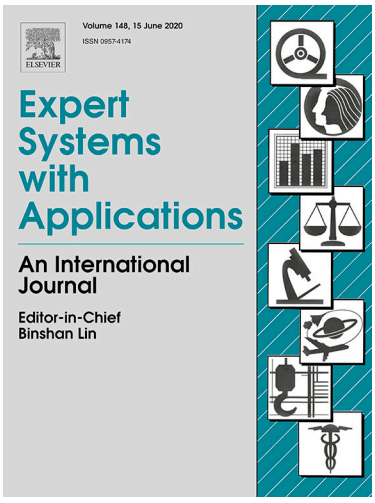

Towards deep probabilistic graph neural network for natural gas leak detection and localization without labeled anomaly data

Xinqi Zhang, Jihao Shi, Xinyan Huang, Fu Xiao, Ming Yang, Jiawei Huang, Xiaokang Yin, Asif Sohail Usmani, Guoming Chen

PII: S0957-4174(23)01044-8
DOI: https://doi.org/10.1016/j.eswa.2023.120542
Reference: ESWA 120542

To appear in: *Expert Systems with Applications*

Received Date: 10 February 2023
Revised Date: 22 May 2023
Accepted Date: 23 May 2023

Please cite this article as: Zhang, X., Shi, J., Huang, X., Xiao, F., Yang, M., Huang, J., Yin, X., Sohail Usmani, A., Chen, G., Towards deep probabilistic graph neural network for natural gas leak detection and localization without labeled anomaly data, *Expert Systems with Applications* (2023), doi: https://doi.org/10.1016/j.eswa.2023.120542

Towards deep probabilistic graph neural network for natural gas leak detection and localization without labeled anomaly data

Xinqi Zhang[1], Jihao Shi[1,2*], Xinyan Huang[2], Fu Xiao[2], Ming Yang[3], Jiawei Huang[1], Xiaokang Yin[2], Asif Sohail Usmani[2], Guoming Chen[1]

[1] Centre for Offshore Engineering and Safety Technology, China University of Petroleum, Qingdao 266580, China

[2] Department of Building Environment and Energy Engineering, The Hong Kong Polytechnic University, Kowloon, Hong Kong, China

[3] Safety and Security Science Section, Department of Values, Technology, and Innovation, Faculty of Technology, Policy, and Management, Delft University of Technology, The Netherlands

[*]Corresponding author

Email address:

Xinqi Zhang: zzxq2020@163.com

Jihao Shi: shi_jihao@163.com, jihao.shi@polyu.edu.hk

Xinyan Huang: xy.huang@polyu.edu.hk

Fu Xiao: linda.xiao@polyu.edu.hk

Ming Yang: M.Yang-1@tudelft.nl

Jiawei Huang: hjw17854217791@163.com

Xiaokang Yin: xiaokang.yin@upc.edu.cn

Asif Sohail Usmani: asif.usmani@polyu.edu.hk

Guoming Chen: offshore@126.com

Towards deep probabilistic graph neural network for natural gas leak detection and localization without labeled anomaly data

Xinqi Zhang[1], Jihao Shi[1,2*], Xinyan Huang[2], Fu Xiao[2], Ming Yang[3], Jiawei Huang[1], Xiaokang Yin[2], Asif Sohail Usmani[2], Guoming Chen[1]

[1] Centre for Offshore Engineering and Safety Technology, China University of Petroleum, Qingdao 266580, China

[2] Department of Building Environment and Energy Engineering, The Hong Kong Polytechnic University, Kowloon, Hong Kong, China

[3] Safety and Security Science Section, Department of Values, Technology, and Innovation, Faculty of Technology, Policy, and Management, Delft University of Technology, The Netherlands

[*]Corresponding author

Email address: shi_jihao@163.com, jihao.shi@polyu.edu.hk

Abstract:

Deep learning has been widely applied to automated leakage detection and location of natural gas pipe networks. Prevalent deep learning approaches do not consider the spatial dependency of sensors, which limits leakage detection performance. Graph deep learning is a promising alternative to prevailing approaches as it can model spatial dependency. However, the challenge of collecting real-world anomaly data for training limits the accuracy and robustness of currently used graph deep learning approaches. This study proposes a deep probabilistic graph neural network in which attention-based graph neural network is built to model spatial sensor dependency. Variational Bayesian inference is integrated to model the posterior distribution of sensor dependency so that the leakage can be localized. An urban natural gas pipe network experiment is employed to construct the benchmark dataset, in which normal time-series data is applied to develop our proposed model while anomaly leakage data is used for performance comparison between our model and other state-of-the-art models. The results demonstrate that our model exhibits competitive detection accuracy (AUC)=0.9484, while the additional uncertainty interval provides more comprehensive leakage detection information compared to state-of-the-art deep learning models. In addition, our model's posterior distribution enhances the leakage localization with the

accuracy of positioning (PAc)= 0.8, which is higher than that of other state-of-the-art graph deep learning models. This study provides a comprehensive and robust alternative for subsequent decision-making to mitigate natural gas leakage from pipe networks.

Keywords: Variation Bayesian Inference; Graph deep learning; Leakage detection; Leakage localization; Digital Twin;

1. Introduction

Global natural gas production and consumption demand have experienced tremendous growth in the past decades since natural gas is considered a 'cleaner fuel source' and burning it produces nearly half as much carbon dioxide (CO2) per energy unit as coal and oil (Gao et al., 2023). In order to meet demand, natural gas transmission and distribution networks have been widely constructed in urban areas, which naturally creates safety issues (Tchórzewska-Cieślak et al., 2018). Natural gas leak from urban pipe networks is among the most severe hazards since the released plume could accumulate into a flammable vapor cloud which, if ignited, can cause a severe fire and/or explosion disaster. To mitigate this risk, real-time automated leakage detection and its location in urban natural gas pipe networks is essential for safe and effective operation and maintenance.

Deep learning has been applied for real-time automated pipeline leakage detection and location (Lindemann et al., 2021). Based on the training approach and the availability of data, these methods could be divided into supervised methods, semi-supervised methods and unsupervised methods. Supervised methods based on models such as artificial neural networks (ANNs) (Esen et al., 2008b, 2009), hidden Markov model (HMM) (Zhang et al., 2021), radial basis function neural networks (RBFNNs) (Song et al., 2022), and convolutional neural network (CNN) (Zheng et al., 2022; Zhou et al., 2021) et al., have been viewed as strong tools for anomaly detection. However, these supervised methods require a large number of labeled anomaly leakage data as training data to achieve acceptable detection accuracy (Korlapati et al., 2022). Since anomaly rarely occurs, collecting adequate volumes of real-world anomaly data is difficult (Spandonidis et al., 2022).

To overcome this limitation, scholars have developed unsupervised and semi-supervised deep learning-based detection approaches. Esen et al. (2017) proposed an adaptive neuro-fuzzy inference system (ANFIS)-based method to decrease the dependency of labeled anomaly data. Tao et al. (2022) proposed a few-shot learning, namely model agnostic matching network (MAMN), for equipment fault diagnosis. Park et al. (2018) and Spandonidis et al. (2022) introduced long short term memory (LSTM) to variational autoencoder (VAE) to construct unsupervised anomaly detection

model. Spandonidis et al. (2022) entailed a long short term memory autoencoder (LSTM-AE) to process signals from accelerometers, providing an unsupervised leakage detection alternative. Although achieving desirable accuracy, the aforementioned approaches ignore the dependency among spatially-distributed sensors, while such dependency may have a significant influence on leakage detection and location accuracy (Ding et al., 2023).

Graph neural networks (GNNs) have become one of the most popular alternatives for anomaly detection and location since GNNs view such networks as non-Euclidean graph structure and capture spatial dependency between nearby graph nodes by introducing an adjacency matrix (Du et al., 2021; Jiang & Luo, 2022). Choi et al. (2021) comparatively analyze state-of-the-art semi-supervised and unsupervised deep-anomaly-detection models, and conducted that GNN-based models were more effective on datasets with dependent time series. Zanfei et al. (2022) applied a graph convolutional neural networks (GCN) and a graph convolutional recurrent neural network (GCRNN) for burst detection in water distribution systems. They compared the performance of the two GCN-based models and highlighted the significant potential of the anomaly detection models learned from a graph structure. Nevertheless, it is worth noting that such graph neural networks are supervised and still require labeled anomaly data for model training. The challenge of collecting real-world anomaly data may compromise GNN performance. With regard to anomaly detection without labeled anomaly data, Deng & Hooi (2021) combined a structure learning approach with GNNs, namely graph deviation network (GDN), additionally using attention weights to explain localization. However, such GNNs apply ‘point-estimation’ approaches such as maximum likelihood estimation (MLE) approach, maximum a posteriori (MAP) expectation maximization (EM), and so on, to optimize the parameters, which may provide ‘over-confident’ detection results even when detection deficiency exists. In natural gas pipeline networks, pressure signals resulting from leakage can be highly fluctuated, leading to larger variation in signal recorded by nearby sensors (Gupta et al., 2018). However, existing GNN-based methods have utilized ‘point-estimation’ techniques to optimize a specific group of neural network parameters and finally estimate the specific results as well. These specific estimations may not reflect the larger variation of pressure signal recorded by sensors more closed to leakage position and thereby affect the leakage localization accuracy of existed GNN-based methods.

Variational Bayesian inference provides a robust alternative by modelling the posterior distribution of parameters inside deep neural networks compared to ‘point-estimation’ approaches (G. Liu et al., 2023; Shi et al., 2021). Variational inference is one of the most well-known alternatives, which replaces the true posterior distribution with an approximate distribution and solves the Kullback-Leibler (KL) divergence between two distributions (Blei et al., 2017; Gal & Ghahramani, 2016). Recently researchers

demonstrated the performance of variational Bayesian inference to estimate the uncertainty of spatiotemporal features and estimation accuracy by incorporating neural networks compared to traditional Bayesian inference such as Monte Carlo simulations etc. (Y. Liu et al., 2020; Shi et al., 2022). Pang et al. (2022) applied variational Bayesian inference to construct a Bayesian spatio-temporal graph transformer (B-STAR) architecture, which achieves state-of-the-art performance in modeling the relationship of multiple agents under uncertainties. G. Liu et al. (2023) proposed a variational Bayesian edge-conditioned graph convolution model to assess the spatial connectivity effects, which exhibited excellent performance with probabilistic prediction reliability on daily streamflow prediction. Although variational Bayesian inference has shown state-of-the-art performance in graph-based probabilistic forecasting, its potential in anomaly detection has yet to be fully explored.

This study aims to propose a deep probabilistic graph learning model for natural gas leak detection and localization without labeled anomaly data. First, the attention-based graph neural network is used to capture spatial dependency among sensors. Then, the variational Bayesian inference is applied to model the larger variation of pressure signal recorded by sensors more closed to leakage position. Besides, a pipeline leakage experiment is conducted to construct the benchmark dataset, using which comparisons between the proposed approach and state-of-the-art models are performed. The major contributions and novelty of this study are listed as follows:

(1) This is the first study to integrate variational Bayesian inference with GNN to model the posterior distribution of dependency weights among spatially-distributed sensors to improve leakage detection and location accuracy in urban natural gas pipe networks without labeled anomaly leakage data.

(2) The experimental study demonstrates our model exhibits competitive detection accuracy while providing uncertainty intervals of leakage detection to support comprehensive decision-making compared to state-of-the-art GNNs.

(3) The experimental study also shows our model provides acceptable overall positioning accuracy, which indicates its higher accuracy for automated natural gas leakage location compared to state-of-the-art GNNs.

(4) This study provides a reliable and accurate alternative for automated anomaly detection and location using GNNs without labeled anomaly data.

This paper is organized as follows: section 2 and section 3 give the mathematical problem and modeling framework of proposed deep probabilistic graph learning. Section 4 presents benchmark dataset constructed by a pipeline leakage experiment. Section 5 and section 6 illustrate the development, validations and comparisons of the proposed model. Finally, limitations and conclusions are provided in section 7 and section 8, respectively.

2. Problem statement

Our task is to improve the accuracy and reliability of automated leakage detection and localization and demonstrate it by comparing it with monitored time-series data collected by spatially-distributed sensors. Existing GNN-based approaches are based on the 'point-estimation' approach and cannot handle uncertainty of detection results. In addition, such approaches locate the leakage position using the single dependency weights among sensors, which are calculated using graph attention learning. The pressure data fluctuates steadily under normal conditions in the natural gas transmission and distribution pipeline system. Once a leak occurs, the loss of fluid will change the fluid density near the leakage location and a rapid pressure drop can be seen. The pressure difference forces the natural gas to squeeze towards the leakage location, establishing a new pressure gradient in the leakage region. The pressure variation in the leakage location is larger compared to areas distant from the leak. Due to the unavoidable stochastic background noise in the pipe network, the pressure fluctuations decay with increasing distance (Gupta et al., 2018). However, the aforementioned dependency weights calculated by prevalent 'point-estimation'-based GNN methods cannot represent pressure variation recorded by sensors near the leakage location.

We aim to model the posterior distribution of dependency weights to present the larger pressure variation nearby and accordingly locate the leakage more accurately by integrating variational Bayesian inference with attention-based GNN. By variational Bayesian inference, we also provide the additional uncertainty of leakage detection. From a mathematical perspective, this is to say we need to model the probability density $P(A|X)$ at time *t*. A is dependency weight among spatially-distributed sensors and X is the previous *s*-steps pressure data monitored by sensors, which can be expressed as:

$$A = \begin{pmatrix} \alpha_{1,1} & \cdots & \alpha_{1,J} \\ \vdots & \ddots & \vdots \\ \alpha_{m,1} & \cdots & \alpha_{m,J} \end{pmatrix} \quad (1)$$

$$X = \begin{pmatrix} x_{1,t-s} & \cdots & x_{1,t-1} \\ \vdots & \ddots & \vdots \\ x_{m,t-s} & \cdots & x_{m,t-1} \end{pmatrix} \quad (2)$$

where m is the number of sensors, J is the number of neighbor sensors of the target sensor.

3. Proposed approach

Fig. 1 demonstrates the architecture of the proposed variational Bayesian inference-graph attention neural network, namely VB_GAnomaly, for real-time automated leakage detection and localization in complex pipe networks.

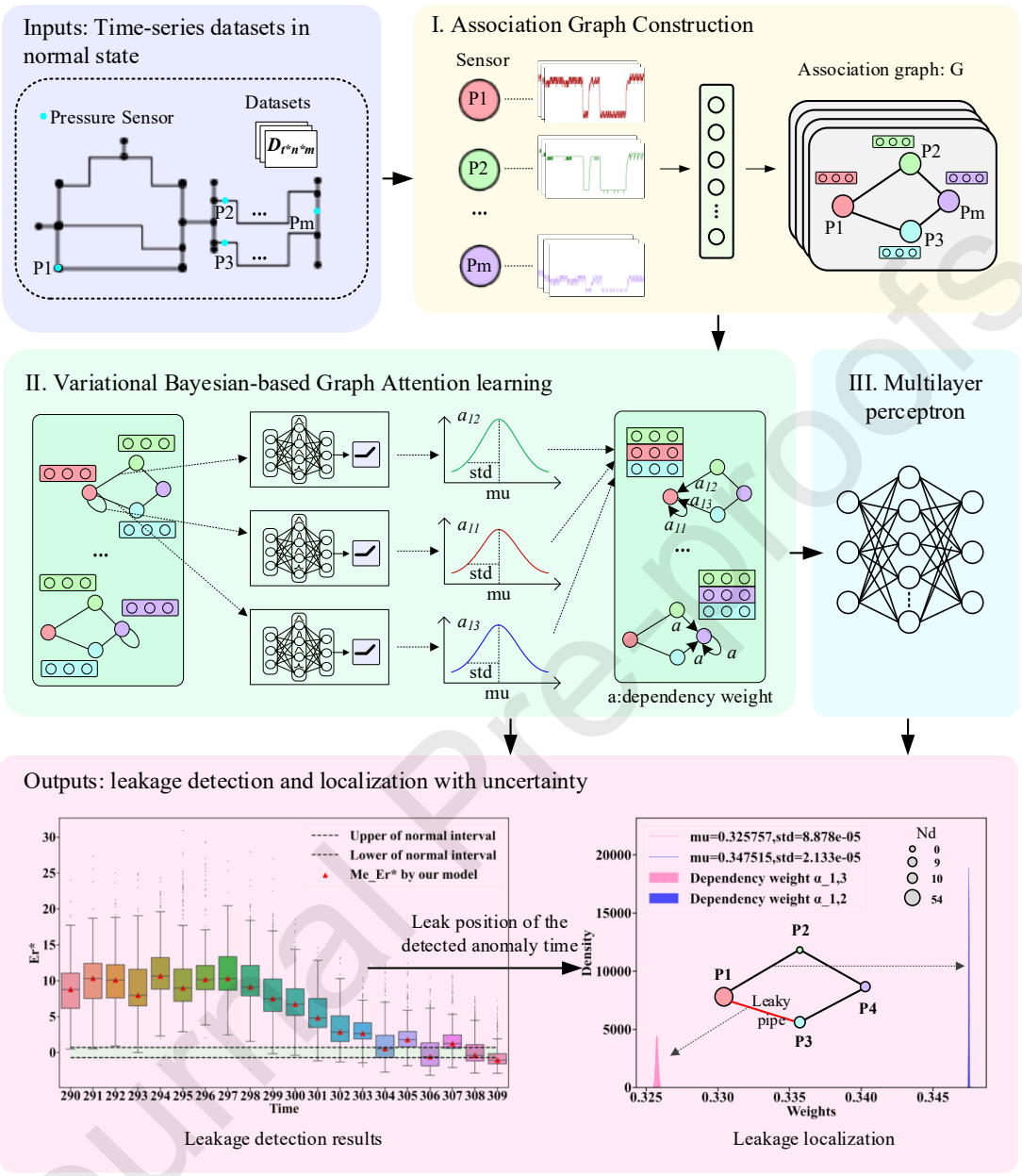

Fig. 1 Architecture of VB_GAnomaly.

3.1 Attention-based graph neural network as the backbone

The attention-based graph neural network is applied as a backbone because the attention mechanism could capture the dependency among spatially-distributed sensors accurately (Choi et al., 2021).

(1) The first part of our proposed VB_GAnomaly is an association graph presenting the connections among sensors of the pipeline network (Hao et al., 2022; Li et al., 2023).

Such connections depend on the flow state such as flow direction, speed etc., inside the pipeline network. We then construct the association graph structure G= (V, E) with nodes V presenting sensors and edges E presenting the connections among sensors. We denote the number of sensors as N_{nodes}= m and the number of connections as N_{edges}= n. We further define the adjacency matrix Ad_{ij} presenting whether connection between sensor i and j exists. In addition, a linear embedding operation is applied to calculate the feature vector v_i of time-series data from sensor i, which can be expressed as:

$$v_i = Embedding^{w_e}([x_{i,t-s}, x_{i,t-s+1},...,x_{i,t-1}]) \quad (3)$$

where $i \in \{1,2,...,m\}$, w_e denotes the parameters in the linear embedding neural layer.

By integrating v_i with time-series data X_i, the initial node representation corresponding to each sensor γ_i can be calculated as:

$$\gamma_i = v_i \oplus w_g X_i \quad (4)$$

where $\oplus$ denotes matrix concatenation and w_g is the weight matrix.

(2) The second part of our proposed VB_GAnomaly is to quantify the connections among sensors by using attention-based neural network. We first apply *LeakyReLU* as the nonlinear activation to determine dependency weights $\xi(i,j)$ between sensor i and its neighbor sensor:

$$\xi(i,j) = attention(i,j) = LeakyReLU\left[w_a^{\top}(\gamma_i \oplus \gamma_j)\right] \quad (5)$$

where w_a is weight vector of learned dependency weights for the attention mechanism, and γ_i, γ_j are the initial node representation of sensor i and sensor j.

Then, we apply the *softmax* function to normalize the dependency weights.

$$\alpha_{i,j} = softmax(\xi(i,j)) = \frac{\exp(\xi(i,j))}{\sum_{k \in \mathcal{N}(i) \cup \{i\}} \exp(\xi(i,k))} \quad (6)$$

where $\alpha_{i,j}$ is normalized dependency weights.

The normalized dependency weights of sensor itself and the weights between sensor and its neighbor sensors are then integrated with feature vector v_i^t of time-series data from sensor i, which can be expressed as:

$$h_i = ReLU\left(\alpha_{i,i} w_g v_i + \sum_{j \in \mathcal{N}(i)} \alpha_{i,j} w_g v_j\right) \quad (7)$$

where h_i is learned node representation.

Subsequently, the set of learned node representations h for all nodes can be expressed as:

$$h = \{h_1, h_2, ..., h_m\} \quad (8)$$

Then, h is regarded as input to a multilayer perceptron layer (MLP) to forecast the pressure $Y = \{Y_1, Y_2, ..., Y_m\}$.

$$Y = MLP^{w_f}(h) \quad (9)$$

where w_f denotes the parameters in the MLP neural layer.

3.2 Variational Bayesian Inference

Variational Bayesian inference is then applied to model the posterior distribution density of dependency weights $P(A|X)$, where A is dependency weight among spatially-distributed sensors and X is the previous *s*-steps data monitored by sensors. Given $\chi = (X, A)$, the probability density $P(A|X)$ can be expressed as:

$$P(A|X) = \int P(A \mid X, w) P(w) dw, w \sim P(w \mid \chi) \quad (10)$$

where w presents a set of parameters in the Linear embedding neural layer and the graph attention deep neural network, $w = \{w_e, w_a, w_g\}$. $P(A \mid X, w)$ denotes the conditional probability density of the dependency weight A given pressure sequence X as well as the parameters w of the deep learning neural network.

According to Bayesian theory, the log probability of $P(w \mid \chi)$ can be inferenced as:

$$\log P(w \mid \chi) = \log\left(\frac{P(\chi \mid w) P(w)}{P(\chi)}\right) \quad (11)$$

$P(\chi \mid w)$ is the likelihood of χ given w, $P(w)$ is the prior probability of initially assumed a list of w values, $P(\chi)$ is the marginal probability.

By using the variational Bayesian inference, an approximate density distribution $Q_\varepsilon(w)$

can be found to represent the posteriori probability $P(w \mid \chi)$. In order to measure the approximation between $Q_\varepsilon(w)$ and $P(w \mid \chi)$, KL divergence is introduced to describe the similarity between both probability distributions, as illustrated below:

$$\begin{aligned} KL(\mathrm{Q}_\varepsilon(w)||P(w \mid \chi)) &= \int \mathrm{Q}_\varepsilon(w)\log\left(\frac{\mathrm{Q}_\varepsilon(w)}{P(w \mid \chi)}\right)dw \\ &= \int Q_\varepsilon(w)\left(logQ_\theta(w) - \log\left(\frac{P(\chi \mid w)P(w)}{P(\chi)}\right)\right)dw \\ &= \int Q_\varepsilon(w)(\log\mathrm{Q}_\varepsilon(w) - \log\left(P(\chi \mid w) - logP(w) + logP(\chi)\right)dw \\ &= logP(\chi) - \int \mathrm{Q}_\varepsilon(w)\log\left(\frac{P(\chi \mid w)P(w)}{\mathrm{Q}_\varepsilon(w)}\right)dw \end{aligned} \tag{12}$$

Since we aim to minimize the $KL(\mathrm{Q}_\varepsilon(w)||P(w \mid \chi))$, and $logP(\chi)$ is a constant that depend on the determined dataset, thus, minimizing the $KL(\mathrm{Q}_\varepsilon(w)||P(w \mid \chi))$ is equivalent to maximizing the second terms of right side. Moreover, given that KL divergence is greater than or equal to 0 (0 if and only if $\mathrm{Q}_\varepsilon(w)$ is equal to $P(w \mid \chi)$), it can be deduced that the second terms of the right side is a lower bound of $logP(\chi)$, donated as, $ELBO$ (Evidence Lower Bound).

$$\begin{aligned} ELBO &= \int \mathrm{Q}_\varepsilon(w)\log\left(\frac{P(\chi \mid w)P(w)}{\mathrm{Q}_\varepsilon(w)}\right)dw \\ &= \int \mathrm{Q}_\varepsilon(w)\log P(\chi \mid w)dw - \int \mathrm{Q}_\varepsilon(w)\log\left(\frac{\mathrm{Q}_\varepsilon(w)}{P(w)}\right)dw \\ &= E_{w\sim \mathrm{Q}_\varepsilon(w)}\log P(\chi|w) - KL(\mathrm{Q}_\varepsilon(w) \parallel P(w)) \end{aligned} \tag{13}$$

where the first term of the right hand is the expectation term of $logP(\chi|w)$ and the second term of the right hand is the KL divergence between $\mathrm{Q}_\varepsilon(w)$ and $P(w)$. Therefore, the variational distribution $Q_\theta(w)$ can be estimated by maximizing the expectation term of $logP(\chi|w)$ and minimizing the KL divergence term $KL(\mathrm{Q}_\varepsilon(w) \parallel P(w))$. Maximizing the expectation term of $logP(D|w)$ and minimizing *MSE* between the predicted and observed pressure values, the first term of the right hand can be expressed as:

$$E_{w\sim \mathrm{Q}_\varepsilon(w)}\log P(\chi \mid w) = -MSE(X,Y) \tag{14}$$

Assuming any distribution could be modeled by multi-Gaussian mixture distributions, we determine $\mathrm{Q}_\varepsilon(w) = PN(\theta,\sigma^2 I) + (1-P)N(0,\sigma^2 I)$ and $P(w) = N(0,\sigma^2 I)$. Then, the KL divergence term $KL(\mathrm{Q}_\varepsilon(w) \parallel P(w))$ can be expressed as:

$$KL(\mathrm{Q}_\varepsilon(w) \parallel P(w)) \approx \frac{\rho}{2}\varepsilon^T\varepsilon - C_1\sigma^2 - C_2 \ln \sigma^2 + C_3 \quad (15)$$

where ρ is the pre-defined dropout probability, ε is the optimized variational parameter, C_1, C_2 and C_3 are constants.

Eventually, the loss function can be minimized by maximizing the expectation term of $logP(\chi|w)$ and minimizing the KL divergence term $KL(\mathrm{Q}_\varepsilon(w) \parallel P(w))$:

$$\begin{aligned} LOSS \approx & -MSE\left(X, \mathrm{VB\_GAnomaly}^{w\sim Q_\varepsilon(w)}(X)\right) \\ & + \frac{\rho}{2}\varepsilon^T\varepsilon - C_1\sigma^2 - C_2 \ln \sigma^2 + C_3 \end{aligned} \quad (16)$$

A stochastic gradient descends (SGD) optimization algorithm is applied to minimize the loss function for the determination of variational distribution $\mathrm{Q}_\varepsilon(w)$.

3.3 Leakage Detection and Localization

Given the new testing input X^*, the posterior distribution $P(A^* \mid X^*)$ can be approximated by $w\sim Q_\varepsilon(w)$, as expressed in Eq. (17):

$$P(A^* \mid X^*) = \int P(A^* \mid X^*, w) Q_\varepsilon(w) dw, \;\; w\sim Q_\varepsilon(w) \quad (17)$$

Further, the Kernel density estimation (KDE) are used to approximate the probability density function (PDF) of the dependency weights A^* (He & Zhang, 2020). Numerous dependency weights can be computed by Monte Carlo (MC) sampling parameters w from the variational distribution $Q_\varepsilon(w)$ in the deep learning of the Eq. (3)- Eq. (6). Accordingly, the predicted pressure can be expressed as:

$$Y^{*1}, Y^{*2}, \cdots, Y^{*mc} = \mathrm{VB\_GAnomaly}^{w^1, w^2, \cdots, w^{mc}}(X^*), w^1, w^2, \cdots, w^{mc} \sim Q_\varepsilon(w) \quad (18)$$

where, mc represents the pre-defined sampling number of our proposed model. Y^{*mc} is the predicted pressure of all sensors under mc-th sampling parameter w^{mc}.

For each predicted pressure Y_i^{*z} of sensor i under z-th sampling parameter w^z, a proportional error Er_i^{*z} can be computed comparing to the observed pressure $X_i^{'}$, as

expressed below:

$$Er_i^{*z} = \frac{|X_i^{'} - Y_i^{*z}|}{X_i^{'}} \quad (19)$$

The mean value of the proportional deviation under *mc* sampling is calculated as the deviation Z_i of sensor *i*, as expressed bellow:

$$Z_i = \frac{1}{mc}\sum_{z=1}^{mc} Er_i^{*z} \quad (20)$$

By comparing the deviation of each sensor, the sensor η^t with the maximum deviation at time t can be obtained. The mc proportional errors of the sensor η^t are sorted according to their values, and the median value of sensor η^t's proportional error $Er_{\eta^t}^*$ is donated as Me_Er^*:

$$Me\_Er^* = \frac{Er_{\frac{mc}{2}} + Er_{\frac{mc}{2}+1}}{2} \quad (21)$$

where $Er_{\frac{mc}{2}}$ is the $\frac{mc}{2}$-th proportional error after sorting.

Then, the proportional error of sensor η^t is compared with the normal threshold to determine whether time *t* is in an anomaly, and the normal threshold $Th(i)$ of sensor i generated by the maximum deviation in validation dataset, which is normal data without label.

Thus, the leakage detection results can be obtained by comparing Me_Er^* with the normal threshold $Th(\eta^t)$ of sensor η^t, which is generated by the maximum deviation in the validation dataset without label. The leakage detection result is expressed as a set of binary labels indicating whether time *t* is leaking or not, i.e. $B \in \{(0,1)\}$, where $B = 1$ indicates that time *t* is leaking. And the detection result B is expressed as:

$$B = \begin{cases} 0 & if \ \_Th(\eta^t) \le Me\_Er^* \le Th(\eta^t) \\ 1 & if\ Me\_Er^* > Th(\eta^t)\ or\ Me\_Er^* < -Th(\eta^t) \end{cases} \quad (22)$$

where $-Th(\eta^t)$ is the lower of the normal interval and $Th(\eta^t)$ is the upper of the normal interval.

Given *mc* sampling proportional errors of sensor η^t, *mc* leakage detection results can be obtained. Our model also gives a probabilistic result of distribution $P(B)$ at time *t,* which can be expressed as:

$$P(B) = \frac{\beta}{mc}^{B} (1 - \frac{\beta}{mc})^{B} \quad (23)$$

where β is the number of anomaly, $0 \leq \beta \leq mc$.

Once an anomaly is detected, the leakage can be positioned according to the uncertainty dependency weights.

The number of maximum deviations for sensor i during the leakage time *T* is donated as Nd_i:

$$Nd_i = \sum_{t=1}^{T} (\eta^t = i) \quad (24)$$

Then, given sensor φ as the sensor with the maximum Nd_i, the standard deviation of dependency weights between the sensor φ and the neighbor sensor *j* is output as $Std_{\varphi,j}$,

$$Std_{\varphi,j} = \sqrt{\frac{\sum_{r=1}^{mc}\sum_{t=1}^{T}(\alpha_{\varphi,j}^{*\,t,r} - \alpha_{\varphi,j}^{*\,mean})}{mc \times T}} \quad (25)$$

Therefore, a maximum standard deviation $Std_{\varphi,\zeta}$ among all the neighboring sensors is calculated, as expressed:

$$Std_{\varphi,\zeta} = \max\{Std_{\varphi,1}, Std_{\varphi,2}, \ldots, Std_{\varphi,j}\} \quad (26)$$

Thus, $Std_{\varphi,\zeta}$ indicating that the position of the edge with the largest weight fluctuation is between nodes φ and , that is, the leak is located between sensor φ and sensor ζ.

3.4 Evaluation metrics for leakage detection and localization

In this work, we use precision (*Prec*), recall (*Rec*), F1-score (F_1), the area under the receiver operating characteristic curve (*AUC*) and the overall positioning accuracy (*PAc*) as the evaluation metrics (Ding et al., 2023). Given the confusion matrix of the predicted results and the true labels of leakage detection, we denote true positive samples, true negative samples, false positive samples, and false negative samples as

TP, *TN*, *FP*, and *FN*, respectively. Precision indicates the percent of positive anomalies to all detected anomalies. Recall is the percent of correctly detected anomalies to all actual anomalies. F1-score can show the trade-off between the value of precision and recall regarding the positive anomalies. Precision, recall and F1-score can be calculated following Eq. (27)–Eq. (29).

$$Prec = \frac{TP}{TP + FP} \quad (27)$$

$$Rec = \frac{TP}{TP + FN} \quad (28)$$

$$F_1 = 2\frac{Prec \cdot Rec}{Prec + Rec} \quad (29)$$

Given K as the number of positive samples and N as the number of negative samples, AUC can be calculated as:

$$AUC = \frac{\sum_{ins_i \in positiveclass} rank_{ins_i} - \frac{K \times (K+1)}{2}}{K \times N} \quad (30)$$

where $positiveclass$ is the set of order numbers of positive samples, and $rank_{ins_i}$ is order number of the i-th sample.

In addition, the overall positioning accuracy is measured by the percentage of leakage that has been correctly localized, as expressed bellow:

$$PAc = \frac{1}{n}\sum_{i=1}^{n} L(E_i,E_i) \quad (31)$$

where the $L(E_i,E_i)$ is the number of samples with a leakage position E_i that are localized in pipeline E_i, n is the number of all the pipelines.

4. Benchmark dataset

4.1 Experimental configuration

A natural gas leakage experiment system of urban gas transmission and distribution pipeline network is used to simulate gas flow with/without leakage. Fig.2 demonstrates

the experimental system, which mainly consists of main pipeline and pipeline branches. The diameter of the main pipelines is 80mm, while the branch pipelines are of diameter 50mm. A gas regulator and several valves are installed in the pipeline network. The gas regulator maintains the inside pressure at 0.1 MPa. 5 ball valves installed at 5 pipeline positions are used to generate 5 gas leakages, namely leak1, leak2, leak3, leak4 and leak5. In addition, pressure signals which are convenient and stable indicators in pipeline leakage diagnosis (Zheng et al., 2020), are used as benchmark time-series data. Four pressure sensors, denoted as P1, P2, P3, and P4 are installed along the main pipeline and branches to collect the benchmark time-series data. The location of each leakage position and the installed sensor are summarized in Table 1. Finally, an online data processing system (DPS) is used to collect the online monitoring time-series pressure signals. The topology graph of experimental pipeline network is constructed with nodes presenting sensors and edges presenting the pipeline connection between sensors, as introduced in section 3.1. The topology graph is shown in Fig. 3.

By using such an experimental system, we monitor the inside pressure for 1 hour and collect 3600=3600s *1 pressure values from each sensor with pressure sampling interval of 1s. Then, we divide all the pressure values into 3590 sequences, each of which includes 10 pressure values. Finally, we generate the benchmark training dataset $X^{train} \in R(4,3590,10)$, without leakage from 4 sensors. For benchmark testing dataset construction, we simulate 5 leakage scenarios by considering 5 leakage positions. For each scenario, we first monitor the inside pressure without leakage for 80s and then set the occurrence of leakage lasting for 80s. Then, we collect 800=5*160 pressure valves, which are divided with 790 sequences and each sequence includes 10 pressure values. Finally, we generate the benchmark testing dataset $X^{test} \in R(4,790,10)$ from 4 sensors.

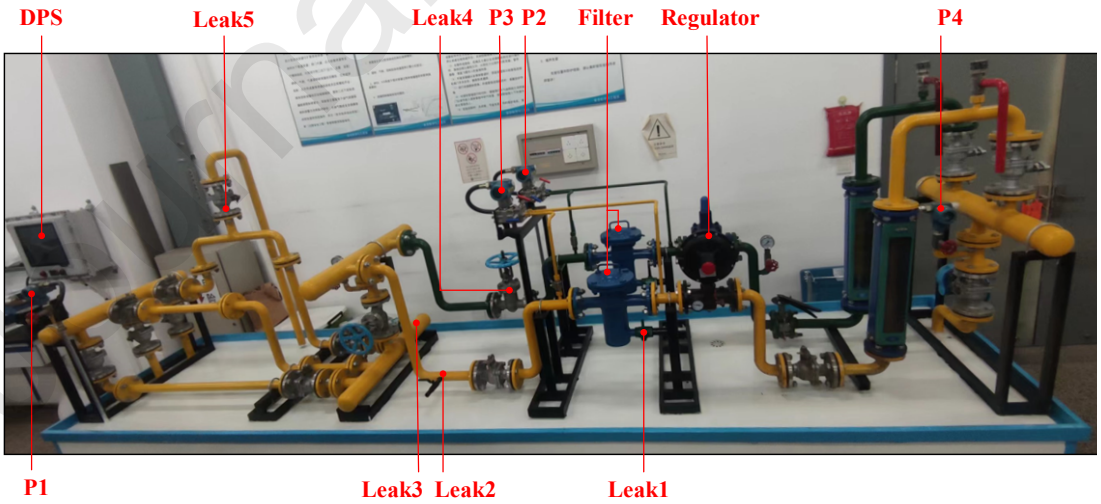

Fig. 2 Lab-scale experimental system of urban gas transmission and distribution pipeline leakage simulation.

Table. 1 Location of the leakage point.

Leak	Upstream sensor	Downstream sensor	Location
Leak1	P3	P4	P3-P4
Leak2	P1	P3	P1-P3
Leak3	P1	P2, P3	P1-P2/P3
Leak4	P1	P2	P1-P2
Leak5	P1	P2, P3	P1-P2/P3

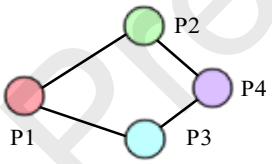

Fig. 3 Topology graph of experimental pipeline network. Nodes present sensors and edges present pipeline connection between sensors.

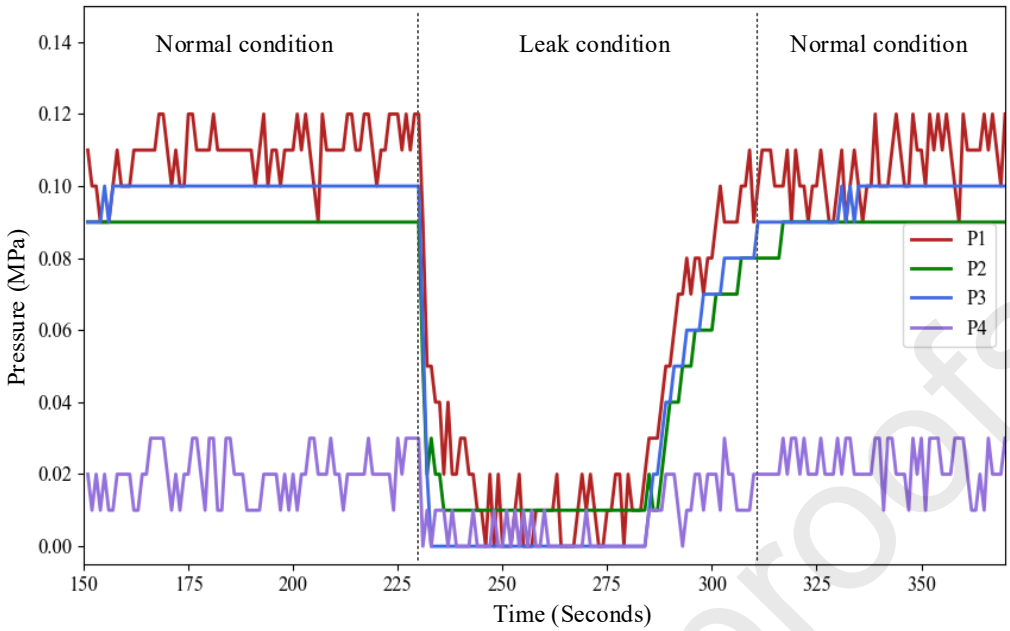

Fig. 4 Time-series pressure data from 4 sensors under pressure 0.1MPa and leak2.

An example of time-series pressure data monitored by 4 sensors under leak2 is presented in Fig. 4. As can be seen, before the occurrence of the leakage, the pressure fluctuates steadily. However, a rapid drop is observed once the leakage is initiated. Among all the sensors, the pressure of P3 shows a larger variance among all sensors, and reaches the lowest pressure of 0 due to its closer location to the leakage position.

4.2 Benchmark dataset processing

Since the experimental pipeline network is composed of pipelines with different pressure grades, i.e., DN50 and DN80, the variation of the monitoring time-series pressure signal among different sensors has a great discrepancy. In this regard, data processing is required to ensure all the monitoring data with the same magnitude in order to accelerate the model's convergence and generalization capability. The min-max normalization approach is adopted to normalize all the time-series data X between 0 and 1 as expressed (Zheng et al., 2020):

$$x_n = \frac{x_l - x_{min}}{x_{max} - x_{min}} \quad (32)$$

where x_n is the normalized value, x_l is the original value, x_{max} and x_{min} are the maximum and minimum of the original values.

5. Probabilistic graph deep learning model development

Our VB_GAnomaly model is compiled by using Python version 3.6 and PyTorch version 1.5.1 with computer server of Intel(R) Xeon(R) Silver 4214R CPU @ 2.40GHz 2.39 GHz and 4 NVIDIA GeForce RTX 2080Ti GPU. Increasing Monte Carlo samples induces the posterior distribution of predicted pressure by Eq.(18) converged, which however increases the computational burden and harms our model's real-time capability for decision-making. Therefore, the trade-off between our model's accuracy and real-time capability should be determined by determining the optimal Monte Carlo *mc* sampling number.

Taking experimental scenario of Leak 1 under inside pressure of 0.1 MPa as example, we first extract 10 groups of weights from variational distribution $Q_\varepsilon(w)$ and accordingly calculate 10 groups of pressure values by Eq.(18). For each group, we extract the weights *mc* times, and then determine *mc* pressure values. This indicates each group includes *mc* predicted pressure values. Fig. 5 displays 10 groups of Cumulative Density Function (CDF) curves of predicted pressure values under *mc*= 50, 300 and 500, respectively. From it, one can see an obvious decrease of the uncertainty interval of predicted pressure value from 0.010564 to 0.005367, as the number of MC samples increases from 50 to 300 when CDF value is 0.5. With further increasing the *mc* number from 300 to 500, such decrease becomes negligible. However, increasing the MC samples would harm our model's efficiency. In this regard, *mc*=300 is selected as the optimal for the trade-off between model's accuracy and efficiency.

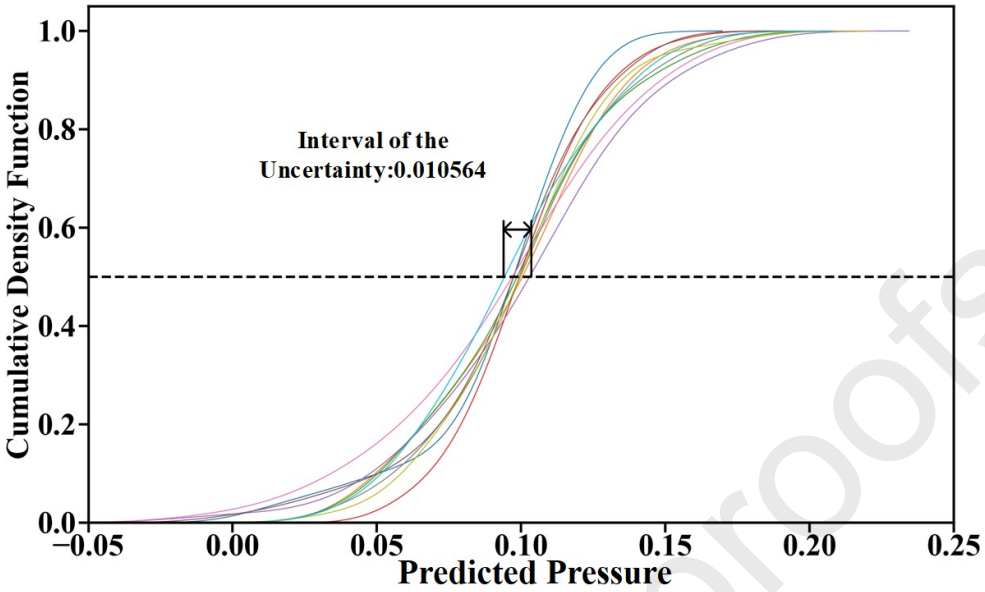

a) 50 samples

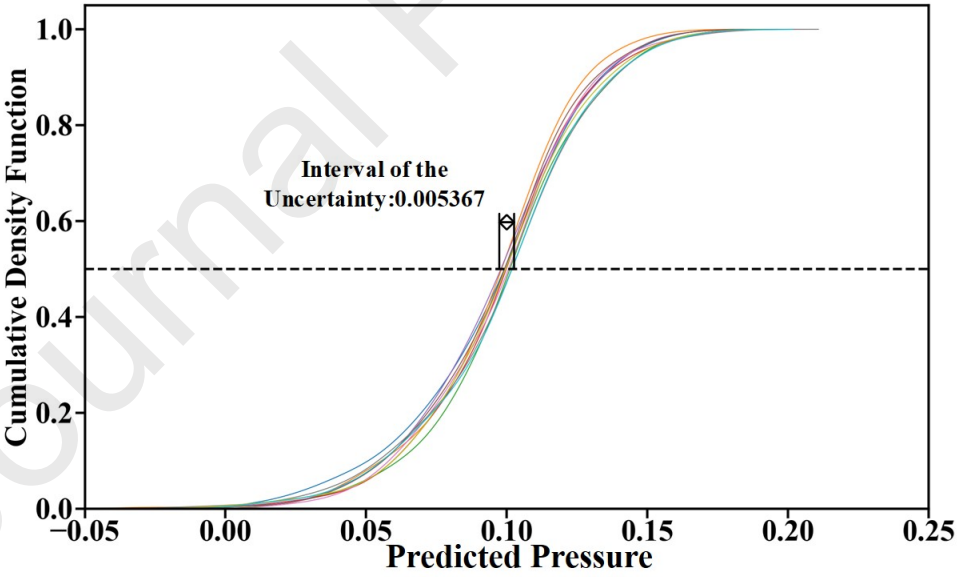

b) 300 samples

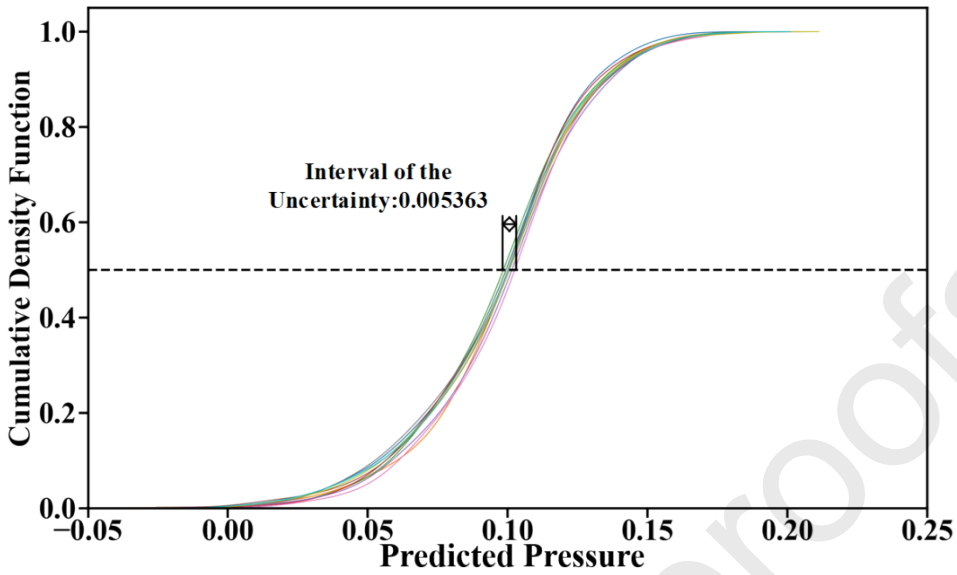

c) 500 samples

Fig. 5 CDF curves of 10 groups of predicted pressure value corresponding to sensor1 under *mc*= 50, 300 and 500.

Fig. 6 displays the probability density function (PDF) distribution of the predicted pressure values of Leak 1 under inside pressure of 0.1 MPa. From it, one can see distribution of the predicted pressure follows the Gaussian distribution with a mean pressure value mu=0.0977 MPa and standard deviation std=0.0288. The difference between the mean pressure value mu=0.0977 MPa and the experimental pressure value 0.10 MPa is 0.0023, indicating our model's accuracy under *mc*=300.

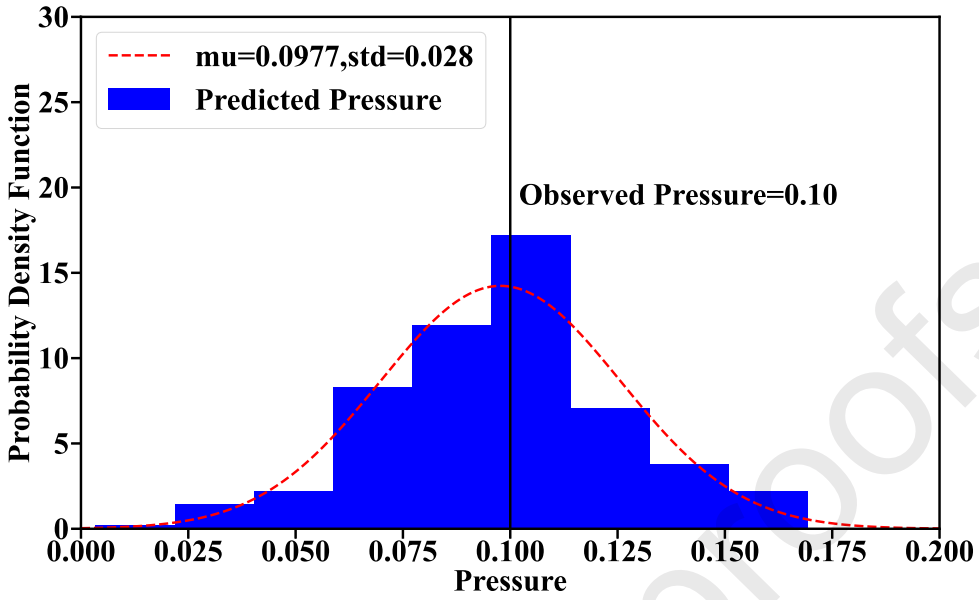

Fig. 6 PDF distribution of predicted pressure under *mc*= 300 corresponding to sensor1.

6. Model validation and comparison

In this section, comparisons between our developed VB_GAnomaly model and six baseline models are conducted to validate our model's accuracy and reliability for leakage detection and localization without labeled anomaly data by using benchmark testing dataset.

6.1 Baseline models

Several neural network-based models on time-series anomaly detection and localization with/without labeled anomaly data are applied as baselines. They are as follows:

(1) ANN (Rostek et al., 2015): An artificial neural network (ANN) consisting of multiple hidden units was applied for unknow attacks detection. Noting that this model requires labelled anomaly data as training data and does not consider the dependency between sensors.

(2) SVM (Esen et al., 2008a): The support vector machine (SVM) model was developed for ground coupled heat pump system performance modeling. This model did not require a pre-knowledge about the system, which means that the model could be trained without labeled anomaly data.

(3) LSTM-VAE (Park et al., 2018): Long short-time memory based variational autoencoder (LSTM-VAE) model was developed for multi-modal sensory anomaly

detection. This model is unsupervised indicating it may not require labelled anomaly data as training data. However, this model also does not consider the dependency between sensors.

(4) GAT (Veličković et al., 2018): Graph attention network (GAT) applied attention-based neural layers to address dependency weights between target node and its neighboring nodes to improve anomaly detection accuracy. GAT is supervised deep graph learning model, which requires labelled anomaly data as training data.

(5) GCN and GCRNN (Zanfei et al., 2022): GCN and graph convolutional recurrent neural network (GCRNN) models were developed and their performance were also compared for anomaly detection in complex water distribution system. These two graph models are supervised and require labelled anomaly data to ensure models' performance.

(6) GDN (Deng & Hooi, 2021): Graph deviation network (GDN) was an unsupervised graph learning model which leverages the self-attention mechanism to quantify dependency weights for anomaly localization.

6.2 Comparison of leakage detection performance

The baseline models are trained by using the default parameters reported in the original paper. Where such parameters are not reported, the parameters employed in our proposed model are adopted to ensure a fair comparison of performance. The specifics include a training epoch of 20, a batch size of 1, and 200 neurons.

Table. 2 demonstrates accuracy comparison of leak detection by using AUC, F1-score, precision, and recall as criterion. From it, one can see that our VB_GAnomaly model has the highest AUC value = 0.9484. Relatively, ANN model has the lowest AUC value = 0.7398 indicating its lowest leakage detection accuracy. This may be attributed to the fact that ANN model cannot accurately learn the spatial dependency between sensors and requires labelled anomaly data for model training process. As an unsupervised model not requiring labelled anomaly data, SVM and LSTM-VAE exhibit a higher AUC value compared to ANN model. However, due to the fact that SVM and LSTM-VAE cannot present the spatial dependency between sensors, its detection accuracy is relatively lower than our VB_GAnomaly model. Although accurately learning dependency features from spatially-distributed sensors, the graph neural network-based models, namely GCN, GCRNN and GAT models, still exhibit lower AUC value compared to our model. The lack of labeled leakage data as training data limits their accuracy. As an unsupervised model which requires no anomaly data and considers the spatial dependency, GDN model has a relatively higher AUC value = 0.9302 compared to the GCN, GCRNN and GAT models. However, GDN model's AUC value is still lower than that of our model. This may be attributed to the fact that GDN mode apply 'point-estimation', which is 'over-confident' when detection deficiency exists. Relatively, our model provides additional detection uncertainty, which effectively avoids detection deficiency.

Table. 2 Leakage detection accuracy of our model and the baselines.

Method	AUC	F1	Prec	Rec
ANN	0.7398	0.6872	0.3727	0.5125
SVM	0.8144	0.6850	0.9155	0.5426
LSTM-VAE	0.8915	0.6429	0.9086	0.4975
GCN	0.7641	0.7246	0.9026	0.6025
GCRNN	0.8356	0.7678	0.9806	0.6325
GAT	0.7619	0.7458	0.9531	0.6100
GDN	0.9302	0.8727	0.8652	0.8825
Our model	**0.9484**	**0.8970**	**0.9013**	**0.8900**

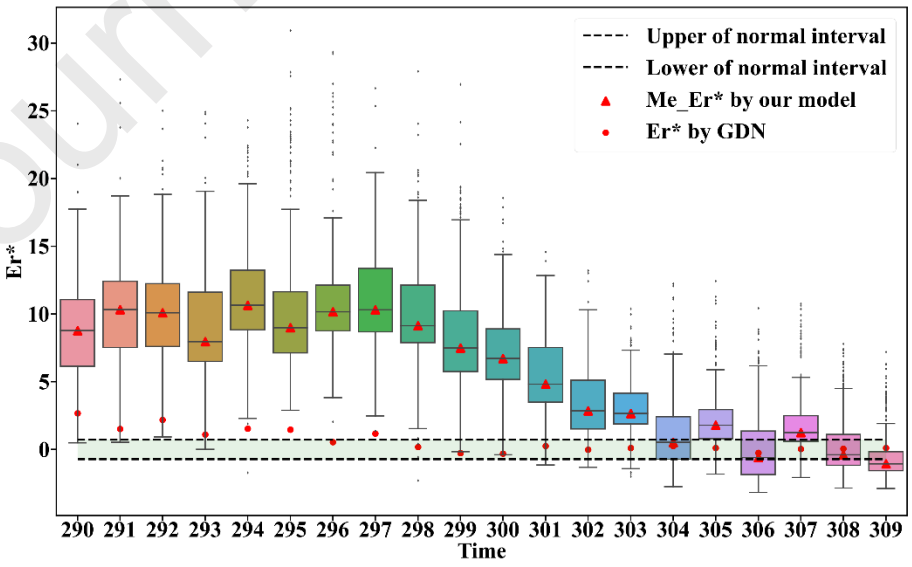

Fig. 7 Leakage detection results of our model and GDN model under leak 2 condition and leakage duration from 290s to 309s. Please noting that Er^* within normal interval indicates model gives the result of no leakage, otherwise indicating leakage occurrence.

To further illustrate our model's higher accuracy over GDN model, the leakage detection curves as shown in Fig. 7 by our model and GDN model under leak 2 scenario and leakage duration from 290s to 309s are used as the example. Please note that the box plot of proportional error Er^* is constructed by first extracting *mc=300* groups of weights from $Q_E(w)$ and then applying Eq.(20) to calculate 300 Er^* values. Also, noting that if Er^* value is located between the upper and lower normal interval, this indicates no leakage exists, otherwise indicating leakage occurrence. From Fig. 7, one may see from 290s to 297s, both of our model and GDN model estimate Er^* values larger than the upper value of normal interval, which indicates both models accurately detect the leakage. However, from 298s to 309s, GDN model provides Er^* values within the normal interval, indicating no leakage exists. This detection result is incorrect since the benchmark experimental scenario includes the leakage. Although estimating the medium value Me_Er^* within the normal interval at, for example t= 306s, our model also provides the additional Er^* values larger than the upper value of normal interval or smaller than the lower value of normal interval due to the variational Bayesian inference. By using Eq.(21), our model gives probability of 58% to identify the occurrence of leakage corresponding to the benchmark experimental scenario. This indicates the variational Bayesian inference can effectively improve our model's detection accuracy even though model's detection deficiency exists. Compared to state-of-the-art models based on the point-estimation approach, our VB_GAnomaly model provides more comprehensive and reliable detection information for follow-up action and decision-making.

6.3 Comparison of leakage localization performance

Among the above six baseline models, only GDN model can be applied to localize the anomaly. Therefore, we further compare our model and GDN model in terms of leakage localization accuracy. Table. 3 demonstrates the comparative results by using the testing dataset. Noting that leak3 and leak5 occur in the main pipeline rather than the branches, as shown in Fig. 2. Taking leak3 as example to clarify, leak3 is located between upstream sensor P1 and downstream sensor P2 and between upstream sensor P1 and downstream sensor P3 as well. It would be correct if our model identifies the leakage position between P1 and P2 or between P1 and P3. If our model identifies leak3 is located between P2 and P3, this estimation would be incorrect.

From Table. 3, one can see our model accurately determines 4 leakage positions among 5 benchmark experimental leakage positions and exhibits higher PAc=0.8. Relatively, GDN model only accurately localizes 1 leakage position and thereby has lower PAc=0.2. This indicates our model's higher accuracy of leakage localization compared

to the GDN model.

Table. 3 Comparison of leakage localization accuracy.

Method	Leak1	Leak2	Leak3	Leak4	Leak5	PAc
Benchmark location	P3-P4	P1-P3	P1-P2/P3	P1-P2	P1-P2/P3	-
GDN	P2-P4	P2-P4	P2-P4	P1-P3	P1-P3	0.2
Our model	P1-P3	P1-P3	P1-P3	P1-P2	P1-P2	0.8

Fig. 8 demonstrates the leakage localization results by our model under leak 2 scenario and leakage duration from 232s to 305s. Fig. 8 (a) shows the number of maximum deviations calculated by Eq.(24) corresponding to each sensor. As can be seen, sensor P1 has the largest number of maximum deviations compared to the additional sensors, which indicates the leakage is in the adjacent pipe of sensor P1. Fig. 8 (b) demonstrates posterior distribution of dependency weights $\alpha_{1,2}$ between sensor P1 and P2, and Fig. 8 (c) shows the posterior distribution of dependency weights $\alpha_{1,3}$ between sensor P1 and P3. As can be seen, the variance of dependency weight $\alpha_{1,3}$ is higher than the variance of dependency weights $\alpha_{1,2}$, which means that the larger variation of monitored time-series pressure data between sensor P1 and P3. We thereby localize the leakage position between sensor P1 and P3, which is corresponding to the benchmark experimental leakage position. Overall, due to the integrated variational Bayesian inference, our developed VB_GAnomaly model can detect and localize natural gas leakage from complex pipe network without any labelled anomaly data.

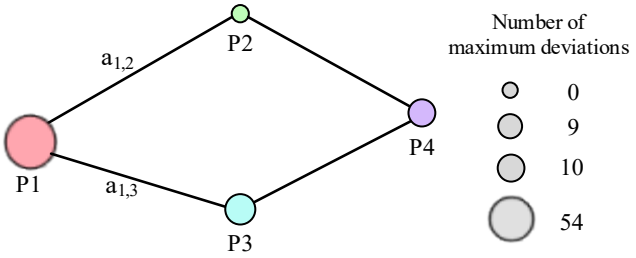

a) Location of the abnormal sensor

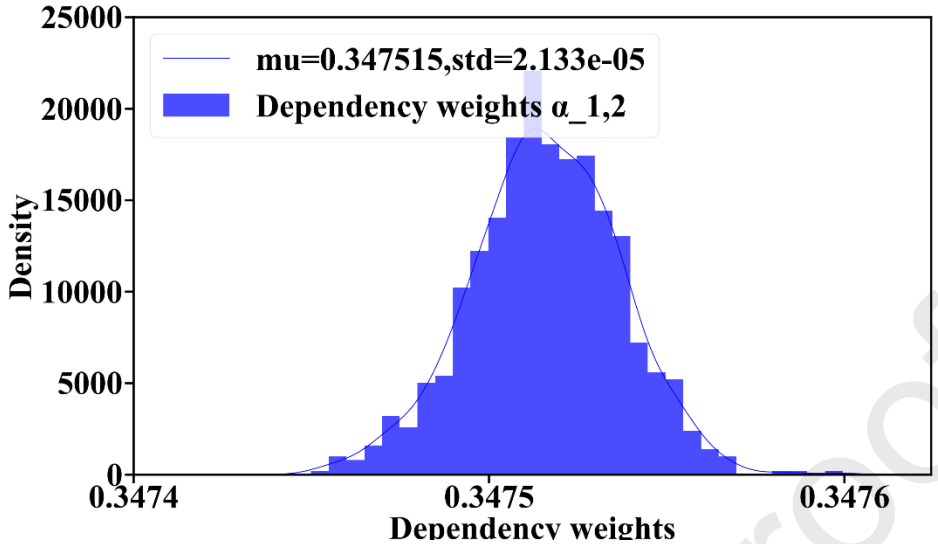

b) Posterior distribution of dependency weights $\alpha_{1,2}$ between sensor P1 and P2

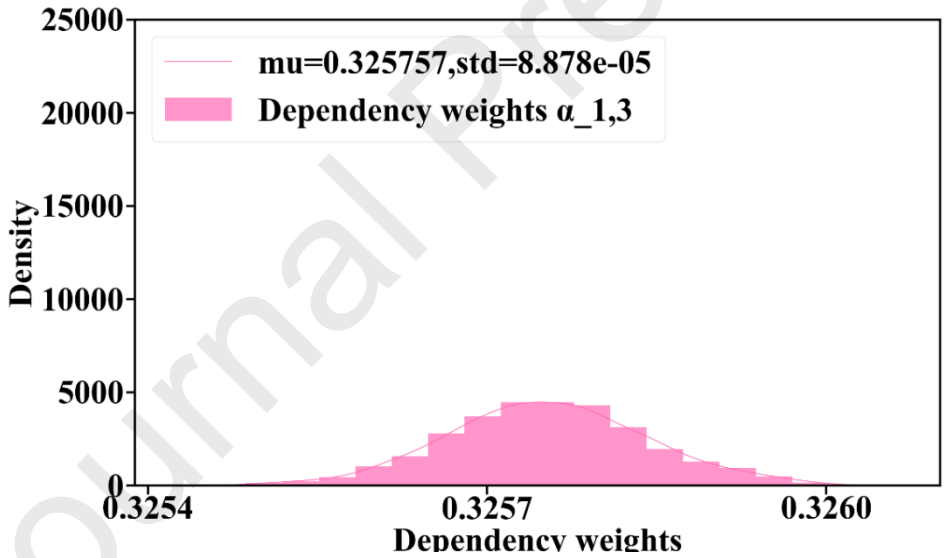

c) Posterior distribution of dependency weights $\alpha_{1,3}$ between sensor P1 and P3

Fig. 8 Leakage localization results.

7. Discussion

This study provides a new idea for anomaly detection in complex system without labeled anomaly data. The proposed model can be implemented for anomaly detection in various domains such as water or gas distribution network, process industry system,

and social network, etc.

Compared to baseline models, the advantages of the proposed model are higher accuracy for leakage detection and localization in urban natural gas pipeline network without labeled anomaly data. This is because that the proposed model could apply the attention-based graph neural network to capture spatial dependency among sensors, making it superior to traditional deep learning-based anomaly detection models. Additionally, compared to existing GNN-based anomaly detection models, the proposed model could utilize the variational Bayesian inference to model the larger variation of pressure signal recorded by sensors more closed to leakage position.

Nevertheless, there are also limitations to be addressed in future work. Firstly, our proposed model was developed by using labor-scale experimental system and cannot be directly applied to real-world full-scale urban pipeline network. This is to say the performance, i.e., inference accuracy and speed of proposed model would be significantly affected by the scale effect of experimental system. For example, the real-world full-scale urban natural gas pipeline network has more sensors. Accordingly, the topology of constructed GNN network for this full-scale pipeline network would be more complex with more nodes, resulting in longer inference time. Future work is expected to investigate this scale effect on proposed model performance.

Secondly, the proposed model outperformed baseline models in comparison with several referenced evaluation metrics, in which the leakage detection evaluation indicators are set according to the anomaly detection studies (Chalé & Bastian, 2022; Ding et al., 2023; Wu et al., 2020), and the leakage localization indicator is set according to the leakage localization indicator in (Quiñones-Grueiro et al., 2018). Besides, there are other indicators about the anomaly detection and localization. The model performance should be further evaluated based on different indicators in future studies.

8. Conclusions

This study proposed a deep probabilistic graph neural network, namely VB_GAnomaly for leakage detection and localization without labelled anomaly data in urban natural gas pipe network. Variational Bayesian inference was incorporated with attention-based graph neural network to model the posterior distribution of dependency weights among spatially-distributed sensors. An experimental study considering various leakage positions was conducted to demonstrate our VB_GAnomaly model's performance. The conclusions were as follows:

(1) Compared to state-of-the-art graph neural networks, our VB_GAnomaly model exhibits higher leakage detection accuracy of AUC=0.9484 and provides additional detection uncertainty intervals for comprehensive and robust decision-making.

(2) Compared to state-of-the-art graph neural networks, our VB_GAnomaly model utilizes variation of dependency weights among sensors to localize leakage and exhibits a higher leakage position accuracy of PAc=0.8.

(3) Overall, our VB_GAnomaly model is expected to provide a robust alternative for constructing a digital twin of operation and maintenance management of urban natural gas pipe infrastructure to accurately detect and localize leaks.

Acknowledgments

This study was supported by National Key R&D Program of China [grant number 2021YFB4000901-03]. National Natural Science Foundation of China (Project No.: 52101341). Natural Science Foundation of Shandong Province (Project No.: ZR2020KF018). China Postdoctoral Science Foundation Funded Project (Project No.: 2019M662469). Qingdao Science and Technology Plan (Project No.: 203412nsh). Key Project of Natural Science Foundation of Shandong Province (Project No.: ZR2020KF018). The authors would like to acknowledge partial support of the Hong Kong Research Grants Council (T22-505/19-N).

References

Blei, D. M., Kucukelbir, A., & McAuliffe, J. D. (2017). Variational Inference: A Review for Statisticians. *Journal of the American Statistical Association*, *112*(518), 859–877. https://doi.org/10.1080/01621459.2017.1285773

Chalé, M., & Bastian, N. D. (2022). Generating realistic cyber data for training and evaluating machine learning classifiers for network intrusion detection systems. *Expert Systems with Applications*, *207*(June), 117936. https://doi.org/10.1016/j.eswa.2022.117936

Choi, K., Yi, J., Park, C., & Yoon, S. (2021). Deep Learning for Anomaly Detection in Time-Series Data: Review, Analysis, and Guidelines. *IEEE Access*, *9*, 120043–120065. https://doi.org/10.1109/ACCESS.2021.3107975

Deng, A., & Hooi, B. (2021). Graph Neural Network-Based Anomaly Detection in Multivariate Time Series. *35th AAAI Conference on Artificial Intelligence, AAAI 2021*, *5A*, 4027–4035.

Ding, C., Sun, S., & Zhao, J. (2023). MST-GAT: A multimodal spatial–temporal graph attention network for time series anomaly detection. *Information Fusion*, *89*(December 2021), 527–536. https://doi.org/10.1016/j.inffus.2022.08.011

Du, G., Liu, Z., & Lu, H. (2021). Application of innovative risk early warning mode under big data technology in Internet credit financial risk assessment. *Journal of Computational and Applied Mathematics*, *386*, 113260. https://doi.org/10.1016/j.cam.2020.113260

Esen, H., Esen, M., & Ozsolak, O. (2017). Modelling and experimental performance analysis of solar-assisted ground source heat pump system. *Journal of Experimental and Theoretical Artificial Intelligence*, *29*(1), 1–17. https://doi.org/10.1080/0952813X.2015.1056242

Esen, H., Inalli, M., Sengur, A., & Esen, M. (2008a). Modeling a ground-coupled heat pump system by a support vector machine. *Renewable Energy*, *33*(8), 1814–1823. https://doi.org/10.1016/j.renene.2007.09.025

Esen, H., Inalli, M., Sengur, A., & Esen, M. (2008b). Performance prediction of a ground-coupled heat pump system using artificial neural networks. *Expert Systems with Applications*, *35*(4), 1940–1948. https://doi.org/10.1016/j.eswa.2007.08.081

Esen, H., Ozgen, F., Esen, M., & Sengur, A. (2009). Artificial neural network and wavelet neural network approaches for modelling of a solar air heater. *Expert Systems with Applications*, *36*(8), 11240–11248. https://doi.org/10.1016/j.eswa.2009.02.073

Gal, Y., & Ghahramani, Z. (2016). Dropout as a Bayesian Approximation: Appendix. *33rd International Conference on Machine Learning, ICML 2016*, *3*, 1661–1680.

Gao, X., Gong, Z., Li, Q., & Wei, G. (2023). Model selection with decision support model for US natural gas consumption forecasting. *Expert Systems With Applications*, *217*(April 2021), 119505. https://doi.org/10.1016/j.eswa.2023.119505

Gupta, P., Thein Zan, T. T., Wang, M., Dauwels, J., & Ukil, A. (2018). Leak detection in low-pressure gas distribution networks by probabilistic methods. *Journal of Natural Gas Science and Engineering*, *58*(April), 69–79. https://doi.org/10.1016/j.jngse.2018.07.012

Hao, J., Liu, J., Pereira, E., Liu, R., Zhang, J., Zhang, Y., Yan, K., Gong, Y., Zheng, J., Zhang, J., Liu, Y., & Zhao, Y. (2022). Uncertainty-guided graph attention network for parapneumonic effusion diagnosis. *Medical Image Analysis*, *75*. https://doi.org/10.1016/j.media.2021.102217

He, Y., & Zhang, W. (2020). Probability density forecasting of wind power based on multi-core parallel quantile regression neural network. *Knowledge-Based Systems*, *209*, 106431. https://doi.org/10.1016/j.knosys.2020.106431

Jiang, W., & Luo, J. (2022). Graph neural network for traffic forecasting: A survey. *Expert Systems with Applications*, *207*(December 2021), 117921. https://doi.org/10.1016/j.eswa.2022.117921

Korlapati, N. V. S., Khan, F., Noor, Q., Mirza, S., & Vaddiraju, S. (2022). Review and analysis of pipeline leak detection methods. *Journal of Pipeline Science and*

Engineering, *2*(4). https://doi.org/10.1016/j.jpse.2022.100074

Li, Z., Yu, J., Zhang, G., & Xu, L. (2023). Dynamic spatio-temporal graph network with adaptive propagation mechanism for multivariate time series forecasting. *Expert Systems With Applications*, *216*(333), 119374. https://doi.org/10.1016/j.eswa.2022.119374

Lindemann, B., Maschler, B., Sahlab, N., & Weyrich, M. (2021). A survey on anomaly detection for technical systems using LSTM networks. *Computers in Industry*, *131*, 103498. https://doi.org/10.1016/j.compind.2021.103498

Liu, G., Ouyang, S., Qin, H., Liu, S., Shen, Q., Qu, Y., Zheng, Z., Sun, H., & Zhou, J. (2023). Assessing spatial connectivity effects on daily streamflow forecasting using Bayesian-based graph neural network. *Science of The Total Environment*, *855*(September 2022), 158968. https://doi.org/10.1016/j.scitotenv.2022.158968

Liu, Y., Qin, H., Zhang, Z., Pei, S., Jiang, Z., Feng, Z., & Zhou, J. (2020). Probabilistic spatiotemporal wind speed forecasting based on a variational Bayesian deep learning model. *Applied Energy*, *260*(December 2019), 114259. https://doi.org/10.1016/j.apenergy.2019.114259

Pang, Y., Zhao, X., Hu, J., Yan, H., & Liu, Y. (2022). Bayesian Spatio-Temporal grAph tRansformer network (B-STAR) for multi-aircraft trajectory prediction. *Knowledge-Based Systems*, *249*, 108998. https://doi.org/10.1016/j.knosys.2022.108998

Park, D., Hoshi, Y., & Kemp, C. C. (2018). A Multimodal Anomaly Detector for Robot-Assisted Feeding Using an LSTM-Based Variational Autoencoder. *IEEE Robotics and Automation Letters*, *3*(3), 1544–1551. https://doi.org/10.1109/LRA.2018.2801475

Quiñones-Grueiro, M., Bernal-de Lázaro, J. M., Verde, C., Prieto-Moreno, A., & Llanes-Santiago, O. (2018). *Comparison of Classifiers for Leak Location in Water Distribution Networks*. *51*(24), 407–413. https://doi.org/10.1016/j.ifacol.2018.09.609

Rostek, K., Morytko, Ł., & Jankowska, A. (2015). *Early detection and prediction of leaks in fl uidized-bed boilers using arti fi cial neural networks*. *89*, 914–923. https://doi.org/10.1016/j.energy.2015.06.042

Shi, J., Li, J., Usmani, A. S., Zhu, Y., Chen, G., & Yang, D. (2021). Probabilistic real-time deep-water natural gas hydrate dispersion modeling by using a novel hybrid deep learning approach. *Energy*, *219*, 119572. https://doi.org/10.1016/j.energy.2020.119572

Shi, J., Xie, W., Huang, X., Xiao, F., Usmani, A. S., Khan, F., Yin, X., & Chen, G. (2022). Real-time natural gas release forecasting by using physics-guided deep

learning probability model. *Journal of Cleaner Production*, *368*(July), 133201. https://doi.org/10.1016/j.jclepro.2022.133201

Song, X., Sun, P., Song, S., & Stojanovic, V. (2022). Event-driven NN adaptive fixed-time control for nonlinear systems with guaranteed performance. *Journal of the Franklin Institute*, *359*(9), 4138–4159. https://doi.org/10.1016/j.jfranklin.2022.04.003

Spandonidis, C., Theodoropoulos, P., Giannopoulos, F., Galiatsatos, N., & Petsa, A. (2022). Evaluation of deep learning approaches for oil & gas pipeline leak detection using wireless sensor networks. *Engineering Applications of Artificial Intelligence*, *113*(March), 104890. https://doi.org/10.1016/j.engappai.2022.104890

Tao, H., Cheng, L., Qiu, J., & Stojanovic, V. (2022). Few shot cross equipment fault diagnosis method based on parameter optimization and feature mertic. *Measurement Science and Technology*, *33*(11). https://doi.org/10.1088/1361-6501/ac8368

Tchórzewska-Cieślak, B., Pietrucha-Urbanik, K., Urbanik, M., & Rak, J. R. (2018). Approaches for safety analysis of gas-pipeline functionality in terms of failure occurrence: A case study. *Energies*, *11*(6). https://doi.org/10.3390/en11061589

Veličković, P., Casanova, A., Liò, P., Cucurull, G., Romero, A., & Bengio, Y. (2018). Graph attention networks. *6th International Conference on Learning Representations, ICLR 2018 - Conference Track Proceedings*, 1–12. https://doi.org/10.1007/978-3-031-01587-8_7

Wu, Z., Pi, D., Chen, J., Xie, M., & Cao, J. (2020). Rumor detection based on propagation graph neural network with attention mechanism. *Expert Systems with Applications*, *158*, 113595. https://doi.org/10.1016/j.eswa.2020.113595

Zanfei, A., Menapace, A., Brentan, B. M., Righetti, M., & Herrera, M. (2022). Novel approach for burst detection in water distribution systems based on graph neural networks. *Sustainable Cities and Society*, *86*(April). https://doi.org/10.1016/j.scs.2022.104090

Zhang, X., He, S., Stojanovic, V., Luan, X., & Liu, F. (2021). Finite-time asynchronous dissipative filtering of conic-type nonlinear Markov jump systems. *Science China Information Sciences*, *64*(5), 1–12. https://doi.org/10.1007/s11432-020-2913-x

Zheng, J., Dai, Y., Liang, Y., Liao, Q., & Zhang, H. (2020). An online real-time estimation tool of leakage parameters for hazardous liquid pipelines. *International Journal of Critical Infrastructure Protection*, *31*. https://doi.org/10.1016/j.ijcip.2020.100389

Zheng, J., Wang, C., Liang, Y., Liao, Q., Li, Z., & Wang, B. (2022). Deeppipe: A deep-learning method for anomaly detection of multi-product pipelines. *Energy*, *259*(July), 125025. https://doi.org/10.1016/j.energy.2022.125025

Zhou, M., Yang, Y., Xu, Y., Hu, Y., Cai, Y., Lin, J., & Pan, H. (2021). A Pipeline Leak Detection and Localization Approach Based on Ensemble TL1DCNN. *IEEE Access*, *9*, 47565–47578. https://doi.org/10.1109/ACCESS.2021.3068292

Credit Author Statement

Xinqi Zhang: Investigation, Methodology, Experiment, Validation, Writing- review & editing.

Jihao Shi: Investigation, Supervision, Methodology, Validation, Writing-reviewing.

Xinyan Huang: Supervision, Writing-reviewing.

Fu Xiao: Supervision, Writing-reviewing.

Ming Yang: Supervision, Writing-reviewing.

Jiawei Huang: Experiment, Validation.

Xiaokang Yin: Supervision, Writing-reviewing.

Asif Sohail Usmani: Supervision, Writing-reviewing.

Guoming Chen: Supervision, Writing-reviewing.